J Mater Sci (2009) 44:129–135
DOI 10.1007/s10853-008-3111-2

Preparation of nanocrystalline Ni–Fe strip via mechanical alloying–compaction–sintering–hot rolling route

S. K. Vajpai · R. K. Dube

Received: 13 June 2008 / Accepted: 10 November 2008 / Published online: 27 November 2008

Abstract Nanocrystalline structures offer opportunity for the development of soft magnetic materials, such as 80 wt% Ni–20 wt% Fe, with superior properties. In recent years, nanocrystalline 80Ni–20Fe (wt%) alloy has been prepared by mechanical alloying of elemental powders. However, retention of nanocrystallinity during consolidation of powder is the key issue to take advantage of improved magnetic properties. In the present work, it has been shown that near-full density bulk nanocrystalline 80Ni–20Fe strip can be prepared via a route consisting of mechanical alloying, cold compaction, sintering, and multi-step unsheathed hot rolling. A crack-free strip of nanocrystalline 80Ni–20Fe, having 99% theoretical density and a grain size of approximately 55 nm, was successfully prepared by sintering and hot rolling of mechanically alloyed powder preforms at 1140 °C. The bulk nanocrystalline 80Ni–20Fe material resulted in a very narrow hysteresis loop indicating a very small hysteresis loss. The present study shows that mechanical alloying–sintering–hot rolling route can be a promising method for producing bulk nanocrystalline materials.

Introduction

A considerable amount of research and development has been carried out for preparing nanocrystalline powder via mechanical alloying. Permalloy (80 wt% Ni, 20 wt% Fe) is a well known soft magnetic material having high permeability, low coercivity, and near-zero magnetostriction [1–3]. The high initial permeability reduces the area of the hysteresis loop considerably, resulting in a very low core loss. The higher resistivity of these alloys makes them suitable for higher frequency applications. In recent years, attempts have been made to synthesize nanocrystalline Ni–Fe alloy powder around the Permalloy composition by mechanical alloying of elemental powders where disordered nanocrystalline Ni_3Fe was found as the major phase [4–7]. Nanocrystalline Ni–Fe alloys synthesized by mechanical alloying have exhibited improved magnetic properties as compared to conventional 80Ni Permalloy. However, not much work has been carried out to consolidate mechanically alloyed powders into bulk form, wherein retaining nanocrystallinity during consolidation to prepare bulk material remains the key issue.

In recent years, a few attempts have been made to consolidate mechanically alloyed powders by several methods, such as vacuum hot pressing [8, 9], explosive compaction [9, 10], hot isostatic pressing [9, 10], spark plasma sintering [11], hot extrusion [12, 13], hot hydrostatic extrusion [14–16], and several combinations of these methods. These methods have been reported to produce near-full density material. However, control over final grain size, uniformity of structure, scale of production, and complexities associated with each of these processing routes remain to be a matter of concern from industrial application point of view. Explosive compaction process seems to be the most attractive process in terms of retaining nanocrystallinity, but complexities associated with the process and final product size restrict its application in large scale. Hot extrusion of mechanically alloyed powders resulted in near-full density compacts having grain size in

S. K. Vajpai (✉) · R. K. Dube
Department of Materials and Metallurgical Engineering, Indian Institute of Technology, Kanpur, Uttar Pradesh 208016, India
e-mail: vajpaisk@iitk.ac.in

R. K. Dube
e-mail: rkd@iitk.ac.in

the range of 0.1 to 1 μm [12–16]. Such a wide range of grain size indicates a lack of control over final microstructure during extrusion. In addition, hot extrusion has been mostly carried out by canning the powder in a suitable container.

The magnetic properties of Ni–Fe materials are strongly dependent on grain size [17, 18]. In such materials, narrow grain size distribution along with nano-sized grains of less than 100 nm grain diameters are crucial to achieve improved functional properties. Recently, consolidation of mechanically alloyed powder involving hot rolling of canned powder was proposed [19]. However, the final grain size achieved by hot rolling consolidation was approximately 1–2 μm. Since mechanically alloyed powder was canned in a stainless steel container before hot rolling, the process became complex and expensive. Hot rolling of uncanned/unsheathed powder preforms in protective atmosphere was developed by Dube and co-workers [20–22], and a variety of metal powder preforms were hot rolled with success. In the present work, a similar processing route for the consolidation of mechanically alloyed nanocrystalline 80Ni–20Fe (wt%) powder by hot rolling has been proposed, which does not require any sheathing or canning of powder preforms. In principle, the route consists of die compaction of mechanically alloyed Ni–Fe powder into a rectangular shape green compact, followed by sintering and multi-pass hot rolling in protective atmosphere. Hot rolling of mechanically alloyed powder preforms in protective atmosphere avoids any oxidation of powder during hot rolling.

The present paper describes the experimental results related to grain size of 80Ni–20Fe material at different stages of processing by the proposed route, viz. mechanical alloying, sintering, and hot rolling. An attempt has been made to optimize the sintering and hot-rolling temperature, together with the total processing time, for optimum grain size and density in the finished crack-free strip. The magnetic properties of the strip are also briefly discussed.

Experimental procedure

Elemental INCO type-123 Ni powder (median particle size = 9.0 μm, composition: C = 600–1000 ppm, O_2 = 600–1000 ppm, Fe < 20 ppm and S = 1 ppm, Ni = balance), electrolytic Fe powder (median particle size = 89.0 μm, >99.9 wt% pure) were used as starting materials. Elemental Ni and Fe powders were annealed in H_2 atmosphere at 700 °C for 30 min for reducing the surface oxides present on the powder. The reduced powder mixture having composition 80Ni–20Fe (wt%) was mechanically alloyed using a high energy planetary ball mill (Fritsch Pulverisette P5). The grinding media were high Ni–Cr steel balls. The disk rotation speed of 450 rpm and the ball-to-powder ratio (BPR) of 8:1 were maintained for the each run. In order to avoid agglomeration, wet milling was carried out using excess acetone as process control agent (PCA). Acetone was added at a regular interval of time to keep the acetone level constant. Samples were collected from the vials after regular time intervals during milling for further investigations.

Rectangular green compacts of mechanically alloyed 80Ni–20Fe powder were obtained by die compaction at a pressure of 400 MPa. Before compaction, the mechanically alloyed powder was mixed with methyl cellulose (2 wt%) and water (1 wt%). The dimensions of the green compacts were 32 mm (L) × 13 mm (W) × 4 mm (T). The density of the green compacts was approximately 45% of the theoretical value. Subsequently, the green compacts were sintered at 700, 800, 900, 1000, and 1140 °C in hydrogen atmosphere for 15 min. During sintering, methyl cellulose evaporated. The hot-rolling temperature was same as the sintering temperature for all experiments. The respective sintered compacts were hot rolled at 700, 800, 900, 1000, and 1140 °C. The sintered compacts were soaked in hydrogen atmosphere at the required temperature for 10 min before hot rolling. The hot rolling was carried out in a specially designed two-high rolling mill interlinked with the soaking furnace in such a manner that the heated sintered compacts remained under protective atmosphere right up to the nip of the mill. The hot-rolled strips were cooled in a bed of charcoal to avoid oxidation. It was possible to hot roll the sintered powder compacts at all the above temperatures to 60% thickness reduction in a single rolling pass. Hot rolling beyond 60% thickness reduction was carried out by multi-pass rolling.

The phase evolution studies and grain size determination of the as-milled, sintered, and hot-rolled material were carried out by X-ray diffraction (XRD) technique using monochromatic Cu K_α (0.154 nm) radiation in a Seifert ISO-DEBYFLEX 2002 diffractometer. The average grain size of the samples was determined by XRD line broadening technique. The measured peak broadening consisted of contributions due to structural (grain refining and strain) and instrumental effects. Therefore, correct average grain size estimation should involve removal of broadening contributions due to instrumental and strain effects from the measured XRD profile. It has been suggested that X-ray peak broadening due to grain size can be represented by a Cauchy function whereas strain broadening can be described by a Gaussian function [23]. Therefore, for mechanically alloyed powders, where both these effects are present, XRD line profile cannot be approximated by solely either by Cauchy or Gaussian function. In such cases, a much better description of the measured structurally broadened XRD line profile can be obtained by an assumed profile shape

which is a convolution of Cauchy and Gaussian functions. The outcome of the convolution of the Cauchy and Gaussian functions is called the Voigt function [23]. This argument will also hold for the instrumental line profile.

In the present work, single line profile analysis procedure based on Voigt function representation was applied for correct average grain size estimation, which takes care of the broadening due to strain and instrumental effects [23]. The most intense peak of the desired phase was considered for grain size determination. The instrumental broadening was corrected using standard silicon powder as reference material. In Voigt technique, the measured line profile '**h**' is considered to be the convolution of the standard profile '**g**' with the structurally broadened profile '**f**' which includes size and strain effects. If **h**, **f**, and **g** are assumed to be Voigt functions:

$$h_C = g_C * f_C \text{ and } h_G = g_G * f_G \quad (1)$$

where subscripts C and G denote the Cauchy and Gaussian components of the respective Voigt profiles.

The integral breadths (β) of f_C and f_G are given by the following equations:

$$\beta_C^f = \beta_C^h - \beta_C^g; \left(\beta_G^f\right)^2 = \left(\beta_G^h\right)^2 - \left(\beta_G^g\right)^2 \quad (2)$$

The constituent Cauchy and Gaussian components of **h** and **g** profiles can be obtained from the ratio $\frac{2w}{\beta}$ where '$2w$' and β are the full width at half maximum intensity (FWHM) and integral breadth of the peak, respectively. In a single line analysis, the apparent grain or domain size D and lattice strain e can be estimated using following set of equations:

$$D = \frac{\lambda}{\beta_C^f \cos\theta} \quad (3)$$

$$e = \frac{1}{4}\beta_G^f \cot\theta \quad (4)$$

where λ is the wavelength of the $K_{\alpha 1}$ radiation used and θ is the Bragg angle for the XRD peak under consideration.

The microstructural features of the mechanically alloyed Ni–Fe powder samples and hot-rolled strips were studied by transmission electron microscope (TEM) and atomic force microscopy (AFM), respectively. The fractured surfaces of the hot-rolled strips were also examined under scanning electron microscope (SEM). Magnetic properties of the hot-rolled 80Ni–20Fe strips were determined by vibrating sample magnetometer (VSM).

Results and discussion

The XRD patterns of the 80Ni–20Fe powder mixture milled for 8, 16, 24, 34, and 46 h together with premixed powder are shown in Fig. 1. The absence of oxide peaks in the XRD patterns of the milled powder showed that the use of excess acetone helped in preventing any appreciable amount of oxidation of powder during ball milling. However, there is always a possibility of contamination of milled powder due to milling media and process control agent (PCA). In the present case, the process control agent (acetone) may contaminate the powder with carbon, whereas milling media (steel balls) with iron. Since iron content in the present alloy system is 20 wt%, an addition of small amount of iron from milling media is not a matter of concern. In addition, no carbon peak was observed in the XRD profile of milled powder. An analysis of the XRD profiles (Fig. 1) shows an increase in the broadening of peaks with increasing milling time. The XRD peak broadening can be attributed to the grain refinement as well as increasing lattice strains with increasing milling time. Another noticeable feature in the XRD patterns is the angular shifting of Ni peaks toward lower angles with increasing milling time. The XRD pattern of 46 h milled 80Ni–20Fe showed that Ni_3Fe was the major phase present in the system. Therefore, the angular shifting of peaks can be attributed to the incipient formation of Ni_3Fe in the system.

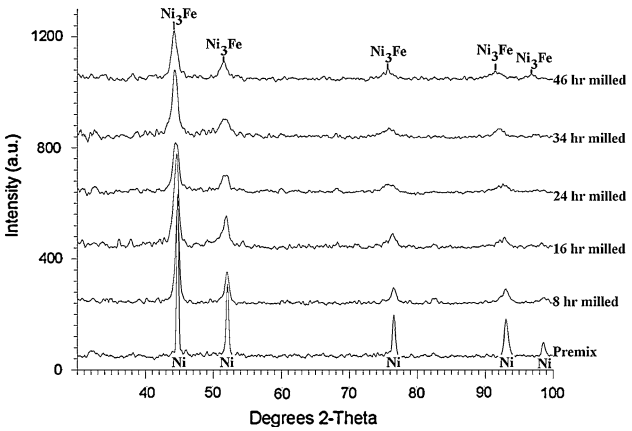

Fig. 1 XRD profiles of premixed and milled 80Ni–20Fe powder

The effect of milling time on the grain size and lattice strain of the resulting Ni–Fe powder is schematically shown in Fig. 2. It can be seen that there was a rapid decrease in the average grain size during initial 8 h of milling followed by a sluggish decrease up to 34 h of milling. The grain size remained almost constant in the range of 34 to 46 h of milling time. The average grain size after 46 h of milling was found to be approximately 15 nm. The lattice strains increased gradually up to 24 h of milling followed by a slight decrease. In the initial phase of milling, accumulation of defects due to severe plastic deformation resulted in severe distortions of the lattice. These defects became localized in the shear bands and

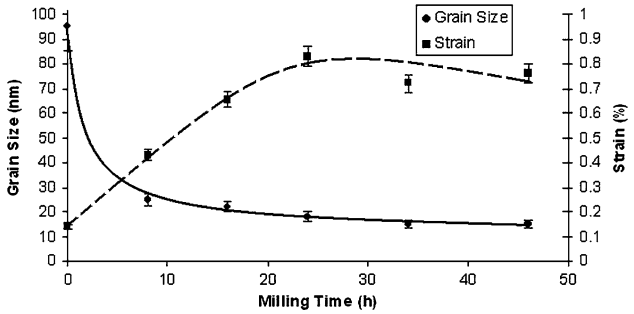

Fig. 2 Variation of grain size and lattice strain as a function of milling time for 80Ni–20Fe

subsequently the structure disintegrated into smaller grains due to higher instability of the structure. Powder milled for 46 h was used for further study in the present work. The morphology of 46 h milled powder is shown in Fig. 3. It can be observed that the milled powder particles were flaky in nature and a few fractured particles were also present. This observation shows that severe plastic deformation together with fracturing of powder particles occurred during ball milling. A detailed TEM analysis of the 46 h milled powder was also carried out. A typical bright field TEM micrograph of the 46 h milled mechanically alloyed 80Ni–20Fe powder and its corresponding SADP of the area are shown in Fig. 4. It can be seen that the microstructure of the mechanically alloyed powder consists of very fine crystalline structure. The grain size from the TEM micrograph was found to be in the range of 5 to 15 nm. The presence of ring pattern in the SADP indicates that the system had a very fine grain structure with randomly oriented grains. Indexing of the SADPs confirmed the presence of Ni_3Fe phase in the system.

As a first step to optimize the hot-rolling conditions for the consolidation of mechanically alloyed powder, the

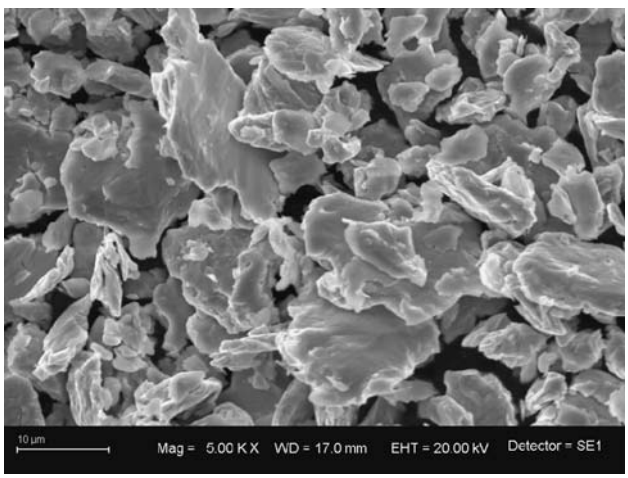

Fig. 3 SEM micrograph of 46 h milled 80Ni–20Fe powder

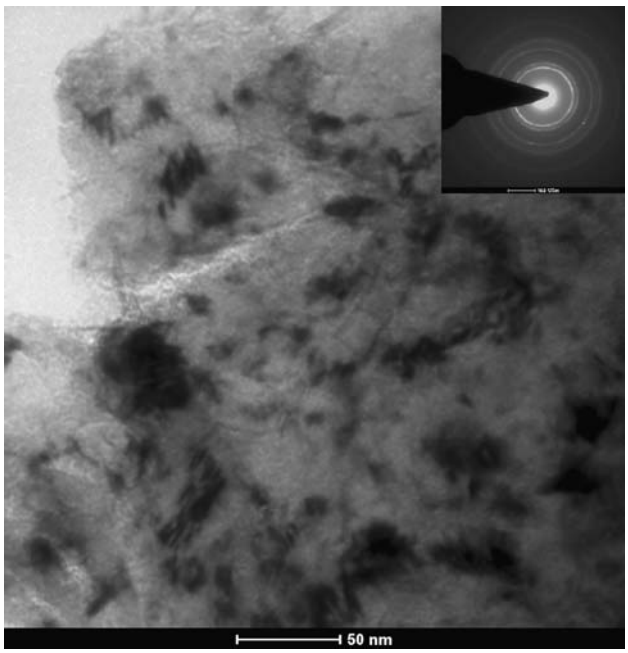

Fig. 4 TEM micrograph and corresponding SADP of 46 h milled mechanically alloyed 80Ni–20Fe powder

green compacts were sintered at different temperatures for 15 min. Subsequently, the sintered green compacts were pre-heated at the same temperature for 10 min, followed by hot rolling to 60% thickness reduction in a single pass. The variation of grain size as a function of hot-rolling temperature is shown in Fig. 5. It can be seen that the grain size increased with the sintering/hot-rolling temperature, showing two regimes of grain growth where the transition temperature lies between 1000 °C and 1140 °C. The presence of two grain growth regimes indicates that

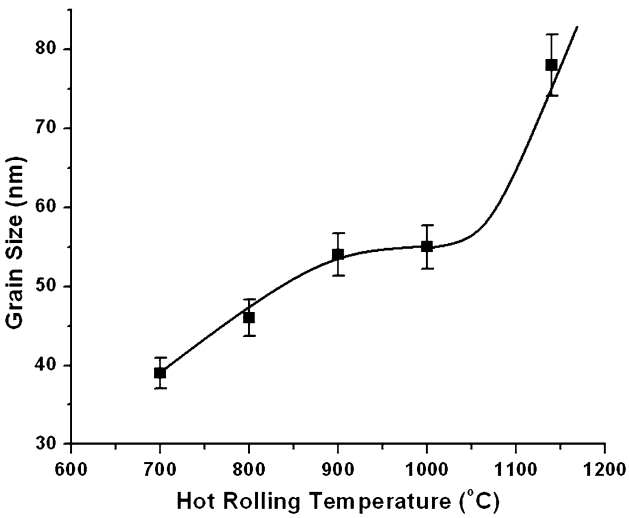

Fig. 5 Variation of grain size as a function of hot-rolling temperature at a constant thickness reduction of 60% for mechanically alloyed 80Ni–20Fe

different grain growth mechanisms are operating in low-temperature and high-temperature regions. In low-temperature region, grain growth is mainly controlled by several factors such as grain boundary diffusion, lattice diffusion, and presence of impurities and solutes [24]. The pinning of grain boundaries by solutes and impurities at low temperatures is considered to be a major factor for retarded grain growth. On the other hand, grain growth at higher temperatures is primarily controlled by lattice diffusion and it does not strongly depend on pinning effects by solutes and impurities. Severe surface and edge cracks were observed in the samples hot rolled in the temperature range of 700 to 900 °C. In case of samples hot rolled at 1140 °C, only minor edge cracks were observed. Therefore, it was decided to use a temperature of 1140 °C for hot rolling in the present study. It has been reported that insufficient interparticle bonding at lower temperatures leads to severe cracking of the hot-rolled strips [25]. However, improved interparticle bond strength was achieved with increasing rolling temperature [25]. Since interparticle bond strength increases with sintering temperature, severity of edge and surface cracks was minimized with increasing sintering/hot-rolling temperature in the present case.

In order to develop an optimum sintering–hot rolling schedule, the grain coarsening behavior of the mechanically alloyed 80Ni–20Fe powder at 1140 °C was studied. The variation of grain size as a function of annealing time at 1140 °C is shown in Fig. 6. It can be seen that rapid grain growth occurs within initial 5 min of annealing followed by a sluggish growth. An average grain size of 50 nm was obtained even after 30 min of annealing at 1140 °C. A similar kind of retarded grain growth kinetics has been reported for nanocrystalline mechanically alloyed Fe–Al alloy [26]. In the present case, the most probable reasons for the retarded grain growth kinetics can be attributed to factors such as stable nanocrystalline structures formed by mechanical alloying, porosity in the milled as well as compacted material, and grain boundary pinning by solutes and other phases such as NiFe. Therefore, if the total time for processing at 1140 °C was kept within 30 min, densification in the strip without excessive grain coarsening can be achieved.

Based on the above results, a three-step sintering–hot rolling of the green compacts, prepared from mechanically alloyed 80Ni–20Fe powder, at 1140 °C was proposed for densification. The total processing time was kept as 30 min. The green compacts were first sintered at 1140 °C for 10 min followed by soaking for 10 min at the same temperature. After soaking, samples were hot rolled to 60% thickness reduction in a single pass. Subsequently, the strips were preheated at 1140 °C for 5 min, followed by a second hot rolling pass to such a thickness reduction which produced a total thickness reduction of 80% w.r.t. initial sintered strip thickness. A similar procedure was used for the third hot rolling step, which resulted in a total thickness reduction of 85% w.r.t. initial sintered strip thickness. Figure 7 shows the grain size variation as a function of thickness reduction by hot rolling of the sintered 80Ni–20Fe samples at 1140 °C. The grain size at zero hot rolling reduction refers to the grain size of the initial sintered mechanically alloyed 80Ni–20Fe green compact. It can be seen that there is a very small grain coarsening during hot rolling step. Most of the grain growth occurred during sintering step. The grain size of the strip after third hot rolling step was estimated to be approximately 55 nm by line broadening XRD technique. The density of the finished

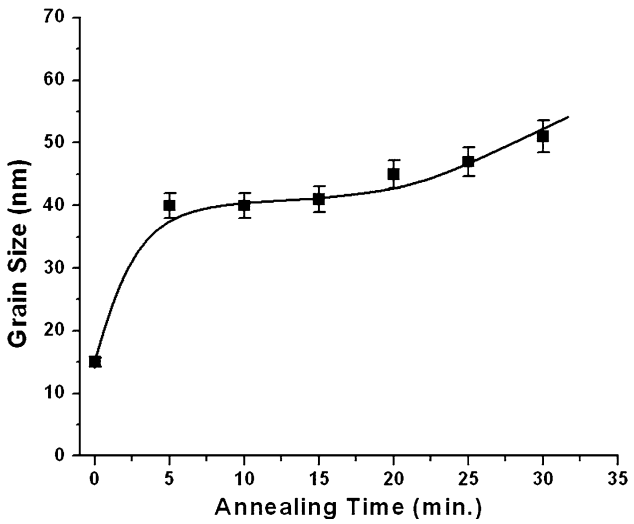

Fig. 6 Grain growth kinetics of 46 h milled mechanically alloyed 80Ni–20Fe powder annealed at 1140 °C

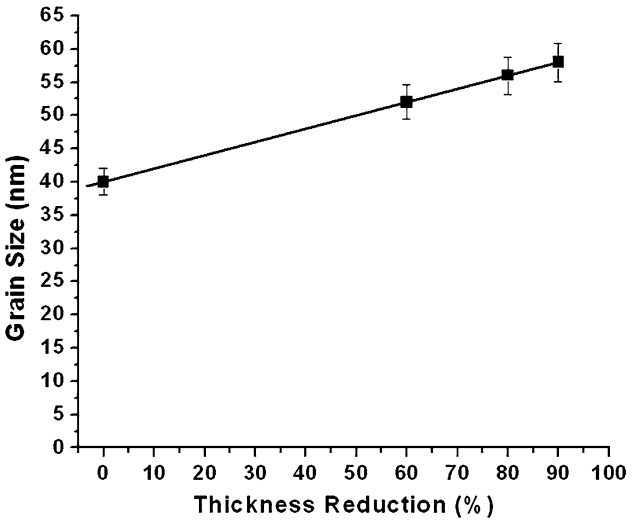

Fig. 7 Variation of grain size as a function of reduction in thickness for 46 h milled mechanically alloyed 80Ni–20Fe hot-rolled at 1140 °C

hot-rolled nanocrystalline 80Ni–20Fe strip was found to be approximately 99% of the calculated theoretical density.

The microstructural features of the hot-rolled bulk nanocrystalline 80Ni–20Fe strip were analyzed by AFM in semi-contact mode. The topographic and phase contrast AFM images of hot-rolled strip on its thickness cross-section parallel to rolling direction are shown in Fig. 8. It can be seen that the elongated nano-size grains are aligned in the direction of hot rolling. The grain sizes of the hot-rolled bulk material along the minor and major axis were estimated in the range of 30 to 50 nm and 40 to 80 nm, respectively. These results show that the multi-step hot rolling has an effect on the shape of the grains and also on the retardation of the grain growth process along the thickness direction. Figure 9 shows the SEM micrograph of the fractured surface of the hot-rolled nano-crystalline 80Ni–20Fe strip. The dimpled surface microstructure

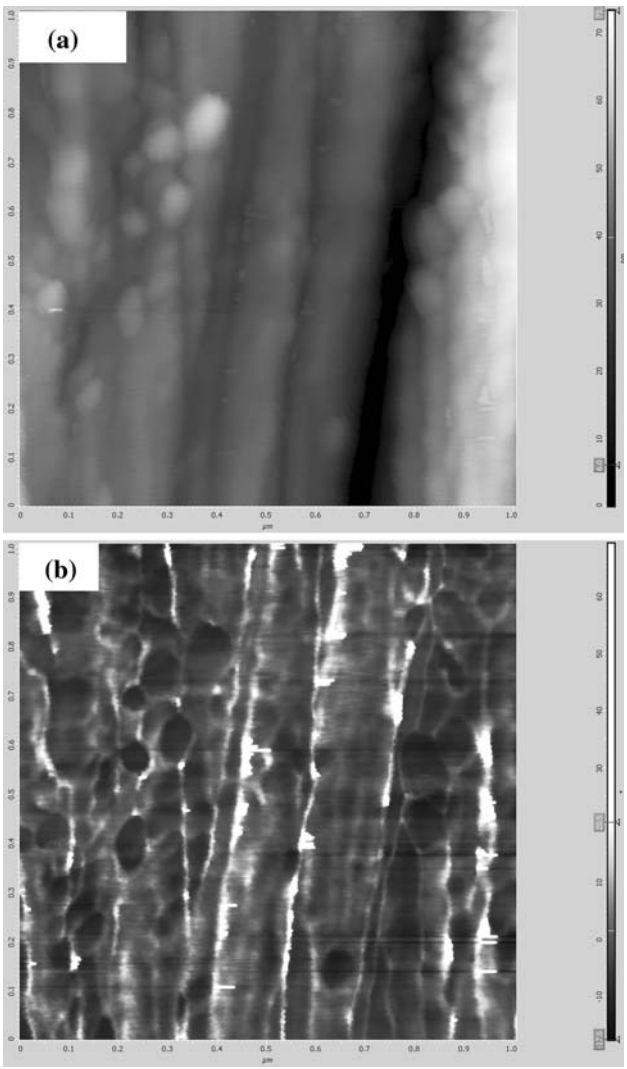

Fig. 8 AFM images of hot-rolled strips **a** surface topographic image **b** phase contrast image

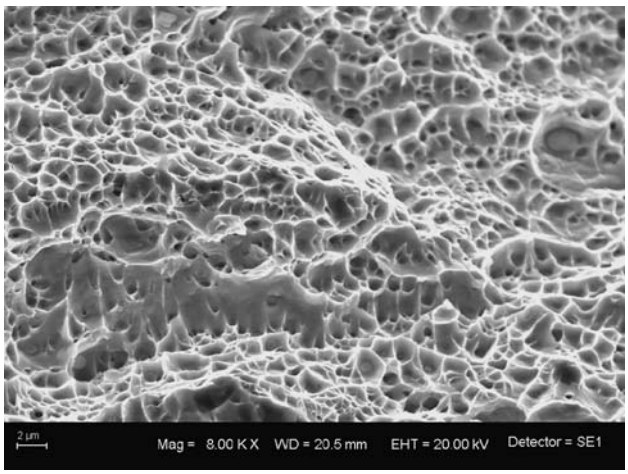

Fig. 9 SEM micrograph of fractured surface of hot-rolled strip

indicates a typical ductile nature of the fracture which confirms an excellent interparticle bonding in the hot-rolled strip. Generally, applications of soft magnetic materials involve frequent reversal of direction of magnetization. Therefore, hysteresis losses must be kept as minimum as possible by controlling the microstructural features, such as dislocations, grain size, texture, precipitates, and order–disorder transformation, etc., to get desired shape of the hysteresis loop [1–3, 17, 18]. The hysteresis curve of the hot-rolled nanocrystalline 80Ni–20Fe strip is shown in Fig. 10. The resulting narrow hysteresis loop implies a very small hysteresis loss under cyclic magnetization field. The shape of the hysteresis loop, indicating high spontaneous magnetization, can be attributed to the disordered structure of Ni_3Fe and textured microstructure of the bulk nanocrystalline strip. The coercive field and saturation magnetization of the bulk hot-rolled strip were approximately 4.42 Oe and

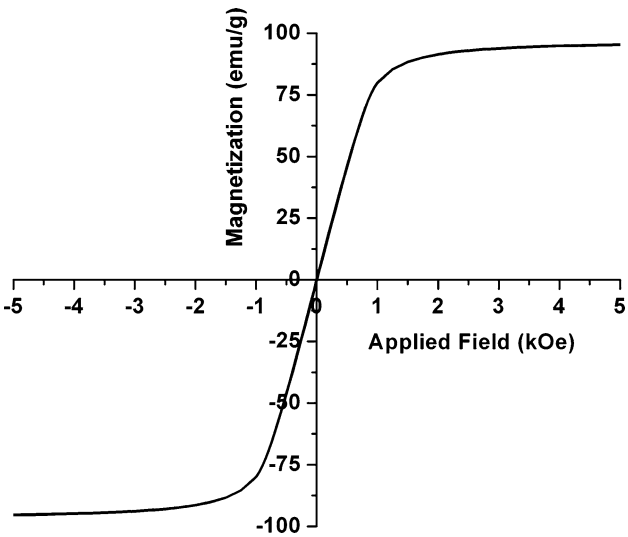

Fig. 10 Hysteresis loop of hot-rolled bulk strip

96 emu/g, respectively, which are similar to the values reported in the literature for comparable grain size [27].

Conclusions

A new processing route for preparing bulk nanocrystalline material from mechanically alloyed powder via compaction–sintering–hot rolling in protective atmosphere has been proposed in the present work. It was possible to prepare near-full density nanocrystalline 80Ni–20Fe (wt%) strip from the mechanically alloyed 80Ni–20Fe powder preforms via sintering–multi-pass hot rolling in protective atmosphere at 1140 °C, keeping the total processing time as 30 min. The grain size of the hot-rolled nanocrystalline strip was found to be approximately 55 nm by XRD line broadening technique. AFM studies revealed the presence of textured microstructure, i.e. elongated grains in the rolling direction, having grain size in the range of 30 to 80 nm. Furthermore, it was found that the multi-step hot rolling had an effect on the shape of the grains and grain growth along the thickness direction of the strip. Hot rolling of the sintered mechanically alloyed nanocrystalline 80Ni–20Fe green compacts in the range of 700 to 900 °C in protective atmosphere resulted in severe surface and edge cracking of the strips. However, only some minor edge cracks were observed when hot rolling was carried out at 1140 °C. A very narrow hysteresis loop was observed for the finished nanocrystalline 80Ni–20Fe strip, suggesting a very small hysteresis loss under reversal of magnetization field direction. The resulting shape of the hysteresis loop was attributed to the disordered structure of Ni_3Fe and textured microstructure of the bulk nanocrystalline sheet.

References

1. Grabbe EM (1940) Phys Rev 57:728
2. Pfeifer F, Radeloff C (1980) J Magn Magn Mater 19:190
3. Couderchon G, Tiers JF (1982) J Magn Magn Mater 26:196
4. Chinnasamy CN, Narayanasamy A, Ponpandian N, Chattopadhyay K, Saravanakumar M (2001) Mater Sci Eng A 304:408
5. Chicinas I, Pop V, Isnard O (2002) J Magn Magn Mater 242:885
6. Shen Y, Hng HH, Oh JT (2004) J Alloys Compd 379:266
7. Isnard O, Pop V, Chicinas I (2005) J Magn Magn Mater 290:1535
8. Choi JH, Moon KY, Kim JK, Oh YM, Suh JH, Kim SJ (2001) J Alloys Compd 315:178
9. Suryanarayana C, Froes FH, Korth GE (1997) Metall Mater Trans A 28:293
10. Korth GE, Williamson RL (1995) Metall Mater Trans A 26A:2571
11. Liu Y, Liu W (2007) J Alloys Compd 440:154
12. Moon KI, Lee KS (1999) J Alloys Compd 291:312
13. Shaw L, Luo H, Villegas J, Miracle D (2003) Mater Sci Forum 426–432:2351
14. Liang G, Li Z, Wang E, Wang Z (1995) J Mater Process Technol 55:37
15. Liang G, Meng Q, Li Z, Wang E (1995) Nanostruct Mater 5:673
16. Wang E, Hu L (2007) Mater Sci Forum 534–536:209
17. Herzer G (1992) J Magn Magn Mater 112:258
18. Herzer G (2005) J Magn Magn Mater 294:99
19. Tsuchiyama T, Hamamoto S, Nakashima K, Takai S (2008) Mater Sci Eng A 474:120
20. Dube RK, Singer ARE (1978) Met Technol 5:270
21. Bhargava S, Dube RK (1986) Mater Sci Technol 2:400
22. Dube RK, Bagdi PK (1993) Metall Trans A 24:1753
23. de Keijser ThH, Langford JI, Mittemeijer EJ, Vogels ABP (1982) J Appl Crystallogr 15:308
24. Malow TR, Koch CC (1997) Acta Mater 45:2177
25. Kodandaram KJ, Bhargava S, Dube RK (1997) Powder Metall 40:37
26. Tang WM, Zheng ZX, Tang HJ, Ren R, Yu YC (2007) Intermetallics 15:1020
27. Frase HN, Shull RD, Hong LB, Stephens TA, Gao ZQ, Fultz B (1999) Nanostruct Mater 11:987